Economical, environmental and exergetic multi-objective optimization of district heating systems on hourly level for a whole year

Hrvoje Dorotić*, Tomislav Pukšec, Neven Duić

University of Zagreb, Faculty of Mechanical Engineering and Naval Architecture,

Department of Energy, Power Engineering and Environmental Engineering, Ivana Lučića 5, 10002, Zagreb, Croatia

Email: hrvoje.dorotic@fsb.hr

Abstract

District heating systems are proven to be an effective way of increasing energy efficiency, reducing the environmental impact and achieving higher exergy efficiency than individual heating solutions. The leaders in district heating integration are Scandinavian countries with more than 50% of the covered total heating demand. Nevertheless, these systems haven't reached their full potential in most European countries. The reason for this could be that energy planners often study only the economic feasibility of the system, thus neglecting other crucial aspects of the previously mentioned district heating. In research papers, district heating multi-objective optimization usually takes into account the minimization of the total discounted cost and the environmental impact. Most times, these two objectives are studied as a single objective optimization problem through the internalization of the cost related to carbon dioxide emissions. This paper presents the multi-objective optimization method which is capable of optimizing district heating technology supply capacities and their operation, including thermal storage, for a one-year time horizon in order to satisfy the optimization goals. The model was written in the open-source and free programming language called Julia, while linear programming solver named Clp was used to obtain the solution. The solver is part of Julia's optimization package called JuMP. Three separate objective functions are included in the model: the minimization of the total discounted cost, the minimization of carbon dioxide emissions and the minimization of exergy destruction. Since these three goals are often in conflict, the final result of multi-objective optimization is the so-called Pareto surface which presents the compromise between all possible results. To deal with the multi-objective optimization problem, the weighted sum method in combination with the epsilon-constraint method was used. The most suitable result has been chosen using the knee point method which is a solution the closest to the Utopia solution where all three goals reach their optimal value.

Keywords: *district heating, exergy, multi-objective optimization, linear programming, thermal storage*

1. Introduction

The fourth generation of district heating (DH) is a concept of an energy system that is capable of integrating power, heating, cooling and even the transport sector [1], [2]. Furthermore, a higher interconnection with active consumers is also expected, thus making them prosumers [3], [4]. Besides sectoral integration, it also implies the reduction of the district heating network supply temperature and the increase of overall system's efficiency [5]. Low-temperature district heating systems will be able to integrate low-temperature renewable energy sources (RES) and locally available low-temperature waste heat [1], [6]. Current systems are still far away from the mentioned goals. Supply temperatures are often higher than 100°C which, by definition, falls into the category of the second generation of district heating systems [7]. However, many researchers are discussing concepts that are even more advanced and put emphasis on exergy analysis. While energy efficiency indicates the effectiveness resource usage, exergy analysis provides the answer on the quality of energy transformation. Space heating temperatures are relatively low when compared to combustion flames in cogeneration plants or boiler units, so from an exergetic point of view, heating demand should be covered by low-temperature sources or excess heat coming from different processes, while high temperature heat should be transformed to useful work, i.e. electrical energy.

The exergy analysis of different network temperatures carried out for Denmark and Swedish systems shows that almost 60% of exergy content in heat supply is dissipated in the distribution system [8]. Another paper also arrived to similar conclusions through a steady-state simulation approach. Authors provided suggestions on how to decrease supply temperature thus increasing energy and exergy efficiency. They concluded that further reduction of exergy destruction is possible for space and domestic hot water (DHW) heating purposes [9]. Gadd and Werner analysed district heating substations' temperature regimes for Danish and Swedish systems and stated that high temperature differences contribute to energy and exergy losses [10]. Exergy has become a common parameter in the analyses of district systems. In her PhD thesis, Şiir Kilkiş developed a rational exergy management model which could facilitate the curbing of carbon dioxide (CO_2) emissions [11]. In another paper, she developed a method for energy planning of near-zero exergy and near-zero compound CO_2 districts [12]. Yang et al. evaluated solutions for DHW demand from low-temperature DH systems [13], while Baldvinsson et al. performed a feasibility and performance assessment of such a system [14]. In some papers, researchers analysed the cost of exergy and integrated it into the exergoeconomic analysis, e.g. by using specific exergy cost (SPECO) method [15].

The previously mentioned papers performed exergy analysis of the system as a whole, while the following ones concentrated on a much more detailed analysis of the district heating system technologies. Yamankaradeniz has performed an advanced exergy analysis for each of the components used in the Bursa geothermal DH system [16]. A similar analysis was carried out in [17] where an artificial neural network modelling was used. Exergy analysis can also be implemented on district cooling systems, as shown in papers [18] and [19]. In the first one, a refuse-derived fuel was analysed, while biomass and solar energy exergy characteristics were assessed in the latter. The exergy of solar and its many applications, including heating, were studied in detail in [20]. Lake and Rezaie are even assessing exergy efficiency of cold thermal storage by means of a detailed simulation and model validation [21]. In paper [22] exergy efficiency analysis of the vapour compression heat pump for heating purposes was carried out.

While analysis and simulation of energy systems can provide detailed information, they can't answer the question: which solution is the most suitable choice? In order to explore this, optimization is needed. Single objective and multi-objective optimization of DH systems has been carried out on different temporal scales, with different possible technologies while taking into account various objective functions such as minimization of total cost [23], [24], [25], minimization of CO_2 emissions [26], minimization of primary energy supply [27] or different combination of mentioned objective functions.

In a case where more than one objective function is defined, a multi-objective optimization approach has to be considered. There are numerous ways to handle this kind of optimization. The most often are genetic algorithms [28], mixed-integer linear programming (MILP) [29] or even non-linear mixed integer linear programming (MINLP) [30]. While many researchers are developing their own algorithms and models, there are also commercially available optimization tools, as the one shown in [31]. Multiple objective functions are usually summed up in a single weighted objective function by using a weighted sum method such as in [28] or [29]. Different approaches could also be used such as epsilon constraint method [32], [33], which is more suited when acquiring the whole Pareto front and not only a single solution of multi-objective optimization.

Exergy-related objective functions are also often included in optimization problems. In [34], exergy isn't specified as an objective function, but exergy destruction is translated into economical loss and integrated in the function. Paper [35] used exergy loss as one of the indicators in a composite utility function. Exergy related parameters such as exergy input, exergy destruction or exergy efficiency are rarely used in single-objective optimization. They are usually part of a multi-objective optimization problem. Franco et al. used second law of thermodynamic in order to reach maximum efficiency of a CHP unit operation in a DH system [36]. Other papers, such as [37] used the maximization of energy efficiency, besides cost minimization, in order to optimize the configuration of organic Rankine cycle. In paper [38], a combined cooling, heating and power cycle was optimized where exergy efficiency, besides total product cost and environmental impact, was chosen as an objective function. Exergy efficiency was also chosen as one of the objective functions in [39], where a net-zero exergy district in China was optimized using a multi-objective optimization approach.

M. Di. Somma et al. in [40] and [41] have optimized a distributed energy system which includes the production of electricity and thermal energy, while taking into account the maximization of exergy efficiency and the minimization of total cost as objective functions. Mixed integer linear programming was used in combination with a weighted sum method in order to handle multi-objective optimization. In [40], only operation of the system was optimized, while in paper [41] supply capacities are also optimization variables. Both papers are considering only representative days, but not a whole year. The time step is equal to one hour. The environmental impact, in terms of CO_2 emissions, wasn't taken into account. Furthermore, the district heating network supply temperature wasn't considered during the calculation of exergy efficiency, i.e. exergy destruction.

Paper [42], published by Dorotić et al, deals with a multi-objective optimization of district heating and cooling systems, while taking into account the minimization of economic and ecological objective functions. The results have shown that for the same discounted cost of the energy system, combined district heating and cooling emits less CO_2 emissions than when operated separately. The model shown in this paper is based on the mentioned research.

In this paper, a multi-objective optimization of district heating systems, which takes into account the minimization of total cost, the minimization of carbon dioxide emissions and the minimization of exergy destruction, was carried out. The model is capable of optimizing the hourly operation and sizing of supply capacities, including thermal storages, for a time horizon of a whole year. Possible supply units include technologies frequently used in district heating systems: air-source heat pump, electrical heater, boiler, cogeneration unit, solar thermal collectors, including short-term and seasonal thermal storage. The model is capable of choosing between using biomass and natural gas as a fuel. The proposed approach is a novelty since such detailed optimization of district heating systems hasn't been reported according to performed literature review. An additional novelty is that exergy destruction is calculated by taking into account the supply temperatures of the district heating network, which can be put in relation with outside air temperature.

Finally, this paper answers the following questions:

1) Which supply technologies should be implemented when shifting from the least-cost solutions to more environmentally friendly and higher quality solutions exergy-wise?
2) How does the change of electricity market prices influence the aforementioned shift?

This paper is structured as follows. Section 2 presents the district heating model and the method used in order to deal with the multi-objective optimization. Section 3 shows a case study of Velika Gorica and the main input data used in this paper. Section 4 shows and discusses the acquired results and provides a discussion. The paper finishes with a conclusion and potential ideas for future work, as shown in Section 5.

2. Method

The method used in this paper is based on the model developed in [42]. It is the multi-objective optimization model used for designing district heating and cooling systems by taking into account the minimization of the discounted cost and carbon dioxide emissions. The model is capable of optimizing supply and thermal storage capacities, including hourly operation for a whole year. The multi-objective optimization problem was handled by using a weighted sum and epsilon constraint method.

For the purposes of this paper, the mentioned model has been improved and updated as follows. First of all, the energy system used in [42] consists of district heating and cooling, while the model used in this paper focuses only on district heating. Secondly, additional thermal storage has been added which is charged only with solar thermal collectors. It could be used as a seasonal storage in a case of large scale integration of solar thermal collectors. Thirdly, the heat pump model has been updated, i.e. the efficiency of the heat pump isn't treated as a constant parameter but is modelled by taking into account the heat source (outside air) and the heat sink (DH network) temperatures. Finally, sink temperature, i.e. district heating supply temperature wasn't taken into account in [42], while its hourly variations have been considered and implemented in this paper.

The major improvement of the model is the addition of the third objective function which is related to exergy and defined as exergy destruction. In paper [42], the final result the of multi-objective optimization was a two dimensional Pareto front, while the main outcome of this paper is a three dimensional front, due to the existence of three objective functions, which shapes a Pareto surface.

Although developed method focuses on optimization of the district heating system from energetic, ecological and exergetic point of view, it is far from life cycle assessment (LCA). First of all, the optimization model covers only one, reference, year in order to optimize system's capacity and operation with a goal to minimize costs, carbon dioxide emissions and exergetic destruction. On the other hand, LCA considers a whole lifetime of each part of the system. Secondly, the method doesn't take into account neither materials nor energy consumed in order to construct the district heating system. Finally, this method doesn't take into account the processes which should be carried out once the supply capacities reach end of their lifetime and need to be decommissioned.

2.1. District heating model

The district heating model used in this paper is shown in Figure 1. The model is capable of choosing between different supply units: heat pump, electrical heater, cogeneration, heat-only boiler, solar thermal collectors and different thermal storages. Two different fuels can be used, natural gas and biomass, while electricity bought on the market drives the power-to-heat technologies, i.e. the electrical heater and the air-water compression heat pump. Cogeneration units are selling electricity on the market, while also receiving feed-in premium in one scenario. Solar thermal collectors have separated storage which acts as a seasonal in a case of high solar fraction. Smaller, short-term thermal storage serves as a buffer for other supply technologies. The district heating network supply temperature

depends on the thermal load, i.e. it is in correlation with the outside temperature, as shown in [7] and [43]. The yearly district heating demand is obtained by using publicly available data [44], while the hourly distribution was acquired by using modified heating-degree hour method in combination with the already known hourly distribution of domestic hot water demand [45].

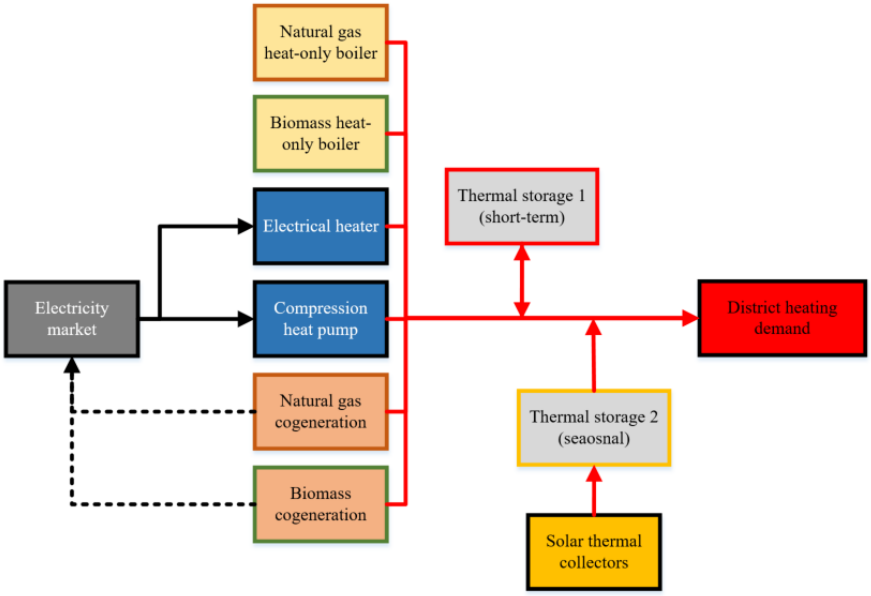

Figure 1 District heating model

2.2.Optimization variables

The optimization is carried out for the following decision variables: the size of supply technologies (P_i), including thermal storages' size (TES_{size}) and solar thermal collector area A_{ST}, and the hourly operation of each technology ($Q_{i,t}$ and $TES_{in-out,t}$) for a whole year. All decision variables are continuous which means the model could be solved by means of linear programming.

2.3. Objective functions

The model falls into the domain of a multi-objective optimization problem, which means that more than one objective function should be used. In this case, three objective functions are defined: the minimization of the total system's cost (economical), the minimization of carbon dioxide emissions (ecological) and the minimization of exergy destruction (exergetic). It is important to note that all objective functions have two summation signs, one for temporal scale (t) and one for technology type (i). The temporal summation is performed in the range from 1 to 8760, i.e. between the first and the last hour of the year.

The economical objective function can be calculated by using Equation 1.

$$f_{econ} = \sum_{i} C_{investment,i} + \sum_{t=1}^{t=8760} \sum_{i} (C_{fuel,i,t} + C_{O\&M,i,t} - Income_{i,t}) \quad (1)$$

Where f_{econ} represents the total discounted cost, i.e. the economical objective function, $C_{investment,i,t}$ is the discounted investment cost of technology i, $C_{fuel,i,t}$ is the fuel cost for technology i in a time step t, $C_{O\&M,i,t}$ is the operation and maintenance (O&M) cost of technology i in a time step t, while $Income_{i,t}$ is the additional income of technology i in a time step t. The last term on the right has a negative sign because it lowers the total cost of the system. An example of income is electricity sold on the market in case of a cogeneration unit. Investment cost doesn't have a temporal summation sign since

it is paid only once, while operational costs (fuel and O&M) and income are paid for every hour of the year.

The ecological objective function can be represented with Equation 2.

$$f_{ecol} = \sum_{t=1}^{t=8760} \sum_{i} (e_{CO_2,i} \cdot Q_{i,t} / \eta_i) \quad (2)$$

Where f_{ecol} is the total system's CO_2 emissions, $e_{CO_2,i}$ is the CO_2 emission factor for technology i, $Q_{i,t}$ is the thermal energy production of technology i for a time step t and finally η_i is the efficiency of technology i. For the purpose of this model, technology efficiency is held as a constant in order to secure the linearity of the model. The only technology with variable efficiency is a heat pump, since it is exogenous variable which depends on the heat source and heat sink temperatures, as explained in Section 2.5.

The exergetic objective function is calculated by using Equation 3.

$$f_{exe} = \sum_{t=1}^{t=8760} \sum_{i} (Ex_{in,i,t} - Ex_{out,i,t}) \quad (3)$$

Where f_{exe} represents the total yearly exergy destruction, $Ex_{in,i,t}$ is the exergy input of technology i in a time step t, $E_{out,i,t}$ is the exergy output of technology i in a time step t. Exergy input and output can be calculated according to the Equation (4) and Equation (5).

$$Ex_{in,i,t} = \frac{Q_{i,t}}{\eta_i} \cdot e_{Exe,i} \quad (4)$$

$$Ex_{out,i,t} = Q_{i,t} \cdot \left(1 - \frac{T_{ref_t}}{T_{DHN_t}}\right) \quad (5)$$

Thermomechanical exergy depends on the thermodynamic properties, i.e. temperature and pressure, of the system and the heat reservoir. For the processes in which there is no chemical reaction, exergy could be expressed by using the temperature of the system and the heat reservoir. However, in order to calculate the exergy of the fuel, chemical exergy shouldn't be neglected. Combustion presents a process in which new chemical species are produced. In order to obtain the total exergy of the fuel, the exergy factor $e_{Exe,i}$ could be used [40], [46] which represents the ratio of exergy and energy of the fuel. It is important to mention that, in some cases, it could be higher than 1. This approach was used in order to calculate the exergy input $Ex_{in,i,t}$, as shown in Equation (4).

In order to calculate the exergy output, only thermomechanical exergy can be taken into account, as shown in Equation (5). Where T_{ref_t} represents temperature of the reference state (outside temperature) in a time step t, and T_{DHN_t} is the supply temperature of the district heating network in a time step t. All the mentioned temperatures are absolute temperatures, expressed in Kelvins. The term in parenthesis in Equation (5) is known as the Carnot factor. The Carnot factor of electricity is equal to one, since it has the highest energy quality. Although exergy destruction minimization is defined as one of the objective functions, exergy efficiency is a parameter which could also be obtained by using Equation (6).

$$\eta_{exe} = \frac{\sum_{t=1}^{t=8760} \sum_i Ex_{out,i,t}}{\sum_{t=1}^{t=8760} \sum_i Ex_{in,i,t}} \quad (6)$$

It is important to mention that exergy efficiency of solar thermal collectors is set to 100%. Although some papers calculate exergy efficiency of solar thermal collectors [20], [40], the authors of this research have decided to assume it is equal to 100%, i.e. there is no exergy destruction in solar thermal collectors. The reason for this is following. Exergy analysis is used in order to evaluate the quality of energy transformation. It is crucial for energy sources which don't have infinite availability such as fossil fuels or biomass. Exergy of these fuels should be utilized as much as possible since they can't be used again once they undergo combustion process. On the other hand, solar energy has unlimited potential. If solar thermal collectors are installed in one energy system, this doesn't limit solar energy utilization in the other energy system. By taking into account exergy destruction of solar thermal collectors, renewable energy sources would be additionally penalized and their successful integration to energy system would have additional obstacle, besides investment cost, to deal with.

2.4. Optimization constraints

District heating system operation must satisfy the thermal demand which is the sum of space heating and domestic hot water (DHW) demand. This constraint could be written as follows:

$$DEM_t = Q_{HOB,gas,t} + Q_{HOB,biomass,t} + Q_{EH,t} + Q_{HP,t} + Q_{CHP,gas,t} + Q_{CHP,biomass,t} - TES_{1,in-out,t} - TES_{2,in-out,t} \quad (7)$$

Equation (7) says that in every hour of the year, the demand DEM_t has to be satisfied with supply technologies ($Q_{i,t}$) and the charge or discharge of thermal storages $TES_{1,in-out,t}$ and $TES_{2,in-out,t}$. As explained in the Section 2.1., two thermal storages are available in the district heating system. Thermal energy of supply capacities can't be larger than its peak power. This can be expressed with Equation (8).

$$0 \leq Q_{i,t} \leq P_i \quad (8)$$

In order to acquire the hourly dynamics of each technology, ramp-up and ramp-down speed constraint is also integrated in the model. This could be written as follows:

$$-r_{up-down,i} \cdot P_i \leq Q_{i,t} - Q_{i,t-1} \leq r_{up-down,i} \cdot P_i \quad (9)$$

Where $r_{up-down,i}$ is ramp-up and ramp-down speed for technology i.

Thermal storage operation is defined with the following set of equations. It is important to mention that these equations could be written for both thermal storages in the same manner.

$$SOC_{t=1} = SOC_{t=8760} = SOC_{start-end} \cdot TES_{size} \quad (10)$$

$$SOC_t = SOC_{t-1} + TES_{in-out,t} - SOC_t \cdot TES_{loss} \quad (11)$$

Where SOC_t is the state of charge of the thermal storage, $TES_{in-out,t}$ is the charge, i.e. discharge of thermal storage, $SOC_{start-end}$ is the predefined state of the charge (expressed as a share) in the first and the last hour of the year, TES_{size} is the thermal storage size, while the product on the right side of Equation (11) represents the thermal storage loss in a time step t which is related to the self-discharge coefficient TES_{loss}. It is important to mention that $TES_{in-out,t}$ has a negative value if the storage discharges and has a positive value if the storage charges. Equation (10) guarantees that thermal storage has the same state of charge in the last hour as in the first hour of the year. For the purpose of this research, $SOC_{start-end}$ for the buffer thermal storage is equal to 50%, while $SOC_{start-end}$ for the seasonal thermal storage is put to 0% since it is charged during the summer season and is completely discharged during winter season. Equation (11) actually presents the energy balance of the thermal storage: the state of charge in the current time step (t), is equal to the state of charge in the previous time step (t-1) increased by thermal storage charge or discharge ($TES_{in-out,t}$) and reduced by thermal storage loss ($SOC_t \cdot TES_{loss}$).

Although the model includes utilization of biomass as a fuel, it is important to notice that there are no constraints put on fuel availability. It means that fuel is always available and can be used for thermal energy production in any hour of the year. This assumption has also been used in other papers dealing with district heating system optimization [40], [45], [47]. However, the model could be easily upgraded in order to include fuel availability constraints.

2.5. Exogenous variables

In the proposed model, there are several exogenous variables: the supply temperature of district heating network, the efficiency of an air-source heat pump, i.e. the coefficient of performance (COP), and specific solar thermal production. Although they aren't constant, they can be acquired prior to the optimization procedure. The supply temperature of the district heating network (T_{DHN_t}) is in correlation with the thermal load, i.e. the outside temperature (T_{ref_t}) [7], [30]. The outside temperature is defined as air temperature on a specific location which could be acquired by using different publicly available databases such as PVGIS [48] or Renewable Ninja [49].

The efficiency of the heat pump depends on the temperature difference between the heat sink and the heat source. For the purpose of this model, the heat pump's heat source is the outside air while the heat sink is defined as a district heating supply network. In order to acquire the efficiency of the heat pump, a modified equation for coefficient of performance is used [45]:

$$\eta_{HP,t} = f_{Lorentz} \cdot \left(\frac{T_{DH,t}}{T_{DH,t} - T_{ref,t}} \right) \tag{12}$$

Where $\eta_{HP,t}$ is the coefficient of performance of the air source heat pump for time step t, which depends on the heat sink ($T_{DH,t}$) and the heat source ($T_{ref,t}$) temperatures, and $f_{Lorentz}$ is known as the Lorentz factor used to acquire the real-life COP from the ideal one [45].

Specific solar thermal collector production depends on solar thermal collector efficiency $\eta_{c,t}$, which could be acquired by using Equation (13).

$$\eta_{c,t} = \eta_0 - a_1 \frac{\left(T_m - T_{ref,t}\right)}{G_t} - a_2 \frac{\left(T_m - T_{ref,t}\right)^2}{G_t} \tag{13}$$

Where η_0 is zero-loss efficiency, also known as optical efficiency, a_1 is first order heat loss coefficient, a_2 is second order heat loss coefficient and T_m is mean solar thermal collector temperature. These parameters are related to solar thermal collector type and could be find in respected specification databases [50]. Finally, G_t is global solar irradiance for ideal azimuth and elevation angles obtained from publicly available databases [7], [30]. It is important to notice that the mean solar thermal collector temperature is taken as a constant, but it is actually a dynamic variable that depends on various parameters such as the thermal load of the solar thermal collector, the mass flow of the medium, etc. This was done in order to secure the linearity of the optimization model. Once the solar thermal efficiency is acquired, the specific solar thermal collector production ($P_{solar,specific,t}$) and the total solar thermal collector output ($Q_{ST,t}$) can be obtained by using Equation (14) and Equation (15).

$$P_{solar,specific,t} = \eta_{c,t} \cdot G_t \tag{14}$$

$$Q_{ST,t} = A_{ST} \cdot P_{solar,specific,t} \tag{15}$$

Where A_{ST} represents the optimal solar thermal collector area, which is the optimization variable related to solar thermal collectors. As can be seen from Equation (15), solar thermal collector operation $Q_{ST,t}$ is constrained.

2.6. Optimization method

As shown in Section 2.3, the proposed method includes three objective functions, which means that it falls into the domain of multi-objective optimization. Equation (16) shows the multi-objective optimization goal.

$$\min(f_{econ}, f_{ecol}, f_{exe}) \tag{16}$$

In this paper, the weighted sum in combination with the epsilon constraint method is used. The weighted sum is one of the most used methods in order to assess Pareto optimal solutions, where all objective functions are merged into single weighted objective function by using weighting coefficients. On the other hand, the epsilon constraint method translates the multi-objective optimization problem into single objective optimization with an additional set of constraints put on other objective functions. Both of the methods are explained and compared in paper [33].

The weighted sum method is shown in Equation (17).

$$F_{weighted} = \left(\frac{\omega_{econ}}{f_{econ_{\omega_{econ}=1}}}\right) \cdot f_{econ} + \left(\frac{\omega_{ecol}}{f_{ecol_{\omega_{ecol}=1}}}\right) \cdot f_{ecol} + \left(\frac{\omega_{exe}}{f_{exe_{\omega_{exe}=1}}}\right) \cdot f_{exe} \tag{17}$$

$$\omega_{econ} + \omega_{ecol} + \omega_{exe} = 1 \tag{18}$$

By using the weighted sum method, the multi-objective optimization problem can be translated into a single-objective optimization by using weighting coefficients ω_i. As can be seen in Equation (17), all three objective functions are summed up and multiplied with the related ω_i, thus composing weighted objective function $F_{weighted}$. Due to the fact that objective functions are usually different order of magnitude, they have to be scalarized by using the optimal value of associated objective function, $f_{i_{\omega_i=1}}$.

The final result of the multi-objective optimization isn't a single value, but a whole set of solutions which lie on a Pareto front. In case of three objective functions, it shapes a so-called Pareto surface. It represent a compromise between three different objective functions. In order to acquire a whole surface, i.e. a solution trend, the weighted coefficients are varied, while the satisfying constraint shown in Equation (18), i.e. their sum has to be equal to one. A major drawback of this method is acquiring the wanted set of solutions on a Pareto surface, especially when having a relatively large step while varying them, e.g. 0,1. Furthermore, the weighted sum method can't provide solutions of the non-convex Pareto fronts, as described in [33].

Once the minimum values of each objective function are known, the boundaries of the Pareto surface are set. Since the goal of this research paper is to acquire a trend, the epsilon constrained method is used to find the other solutions of the Pareto surface. This method allows the translation of a multi-objective optimization problem into a single objective optimization problem with an additional set of constraints. This is shown on the example of a minimizing economical objective function with constraints put on exergy destruction and carbon dioxide emissions, Equation (19). By increasing or reducing a specific constraint, additional solutions are acquired and the Pareto front can be fully visualized. In this way, the front with equally spaced points can be constructed which is then used for further analysis. A major drawback of this method is the necessity of running a large number of optimizations in order to obtain the Pareto surface with an acceptable level of detail. Furthermore, before using this method, the end-user should know the boundaries of the Pareto surface, since the epsilon constraint should be defined in the feasible region of solutions [33].

$$\min\,(f_{econ}) \text{ for } f_{ecol} = \varepsilon_{ecol}\,, f_{exe} = \varepsilon_{exe} \tag{19}$$

2.7. Obtaining the most suitable solution

Finally, in order to choose the most suitable solution on the Pareto surface, decision making should be carried out. While various different approaches exist, in this paper the most suitable solution is defined as the one closest to the Utopia point. The Utopia point is an ideal, but unfeasible solution where all three objective functions achieve their optimal values. Mathematically speaking, the most suitable solution is the one with the least distance to Utopia point, as shown in Equation (20) and Equation (21).

$$\min(P_{solution}) \tag{20}$$

$$P_{solution} = \sqrt{\sum_{j} (f_{j_{Utopia}} - f_j)^2} \tag{21}$$

Where $P_{solution}$ is the distance to the Utopia point, $f_{j_{Utopia}}$ is the minimum possible value of normalized objective function j and f_j is the non-minimum value of normalized objective function j. This method is also known as the knee-point method and it could also be used in a multi-objective optimization problem when two objective functions are defined.

3. Case study

The method was tested on the town of Velika Gorica (45°43'11,9"N 16°04'19,3"E), located in Zagreb County, Croatia. Total area of Velika Gorica is equal to 552 km^2, while urban area is equal to 31 km^2. The town has population of 30.000 while the municipality has around 60.000 inhabitants. The town itself has 14 small district heating system with the overall capacity of 70 MW and around 50.000 MWh of thermal energy distributed to final customers with a thermal network efficiency equal to 80%. Most of the existing smaller DH systems covers both space heating and DHW demand. In the scope of this research, the analysis of replacing part of the district heating supply system was carried out. Furthermore, it is planned that new system would also cover domestic hot water demand and operate through a whole year. The total space heating demand of the final customers connected to that part of the system is equal to 23.000 MWh. According to [45], DHW share in the total household thermal energy demand in Eastern European countries is around 15%, while for highly insulated dwellings in Northern Europe it doesn't drop below 40%. For the purpose of this case study it is assumed that the DHW share for Velika Gorica is 10%, i.e. equal to Croatian's average share of DHW [51].

3.1. Input data

The hourly distribution of space heating was obtained by using the degree-hour method, while the hourly DHW demand was acquired by using the already known existing relative distributions [45]. Figure 2 shows the district heating load obtained by using the modified heating-degree hour method and includes space heating and DHW demand, including thermal network losses. It can be seen that the load has a highly seasonal effect with the peak demand equal to 19,7 MW during winter season, while the summer load usually isn't higher than 1 MW. Furthermore, it is assumed that the DH system doesn't provide thermal energy to the network during the night, i.e. from 22:00 in the evening until 05:00 in the morning. A more detailed hourly distribution of the heating demand can be seen in the Section Results.

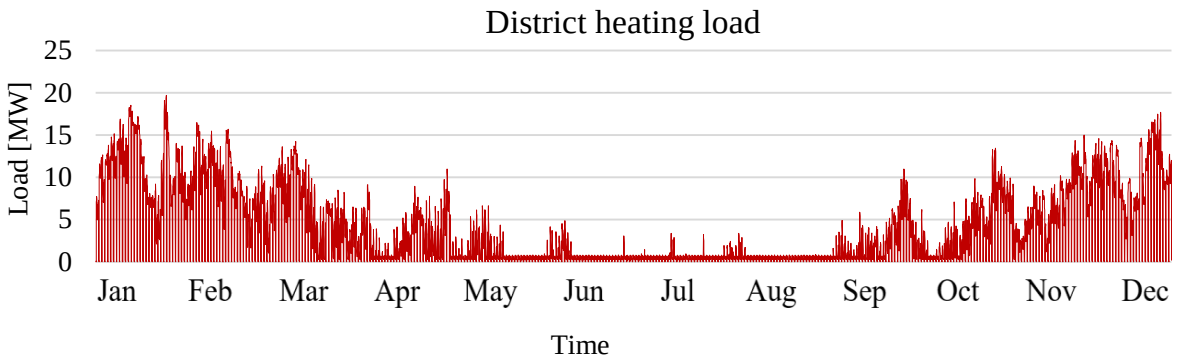

Figure 2 District heating load

The meteorological data for the location of Velika Gorica [52], which is used for the calculation of exogenous variables and the hourly district heating demand distribution, is shown in Figure 3. The maximum outside temperature is 36 °C while the minimum is equal to -10 °C. Temperature distribution data is needed for calculation of compression heat pump COP and the district heating supply temperature. The maximum global solar irradiation is equal to 1.180 W/m^2, while the average is equal to 156,3 W/m^2. This makes this location suitable for solar thermal collector integration [53].

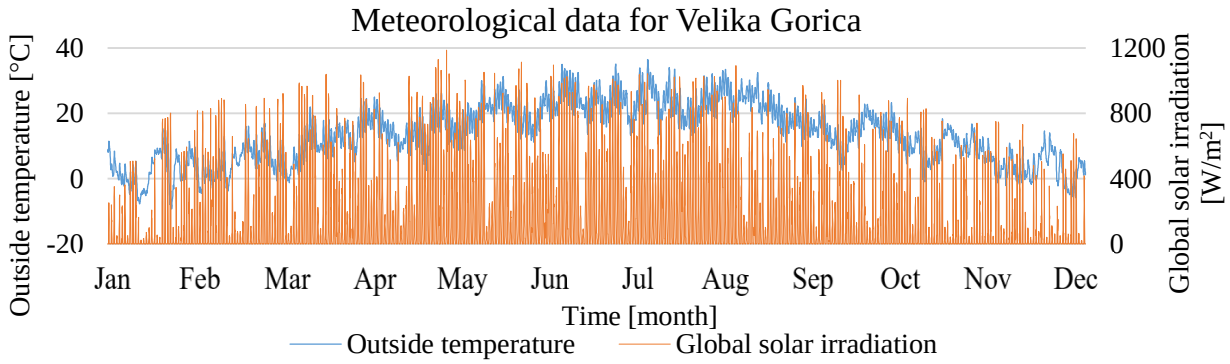

Figure 3 Meteorological data for Velika Gorica

Since the exact supply temperature of district heating systems depends on various parameters [7], it was assumed that existing infrastructure operates as third generation district heating. The reason for this is a relatively low household specific heating demand equal to 155,95 kWh/m^2 and a relatively short thermal network [44]. It is assumed that the maximum supply temperature is 100°C, while the minimum supply temperature is set to 60°C in order to satisfy the domestic hot water demand during the summer season. The relation between the district heating supply temperature and the outside temperature, including the equation of the slope in the diagram, is shown in Figure 4. As explained in the section on the Method, the district heating supply temperature is used to calculate the heat pump efficiency, and the exergy destruction. Since it depends on the outside temperature, the supply temperature is also an hourly distribution.

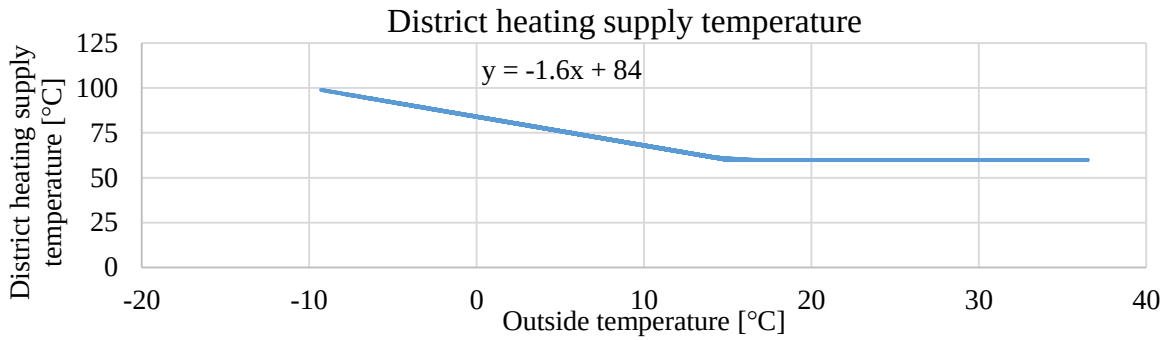

Figure 4 District heating network supply temperature as a function of outside temperature

The coefficient of the performance of the air source heat pump used in the model is shown in Figure 5. As discussed in Section 2.5, it is a function of the district heating supply and the outside (reference) temperature. It is important to note that minimum COP values are obtained during the winter season, while the maximum efficiency is achieved during the summer season, i.e. when the district heating load is lower. The average COP is equal to 2,103. This has a great influence on the multi-objective optimization results, as explained in Section 4.

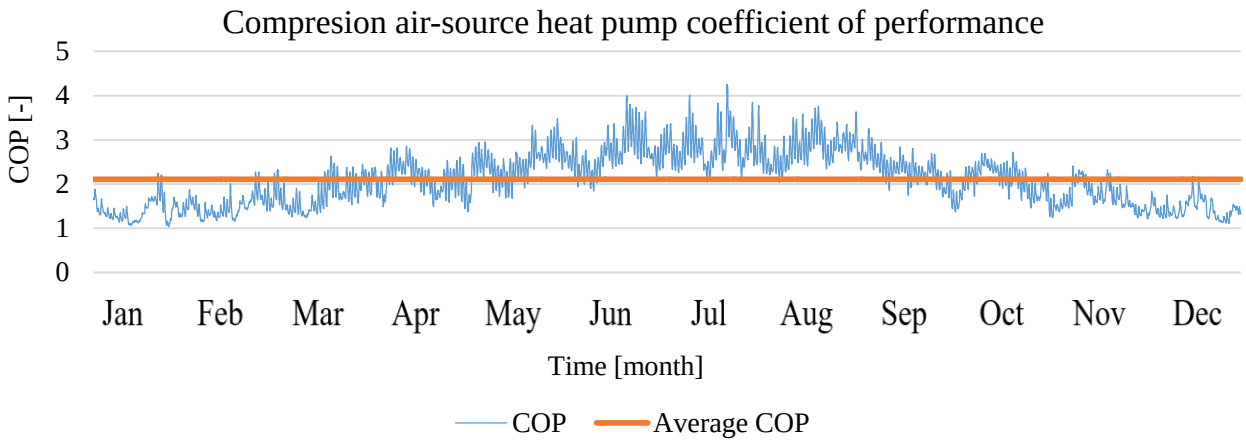

Figure 5 Coefficient of performance of the air-source compression heat pump

The specific solar thermal collector output is shown in Figure 6. The maximum output is obtained during the summer season and it is equal to 600 W/m^2. Due to the low temperatures during the winter season, the output from solar thermal collectors is often equal to zero.

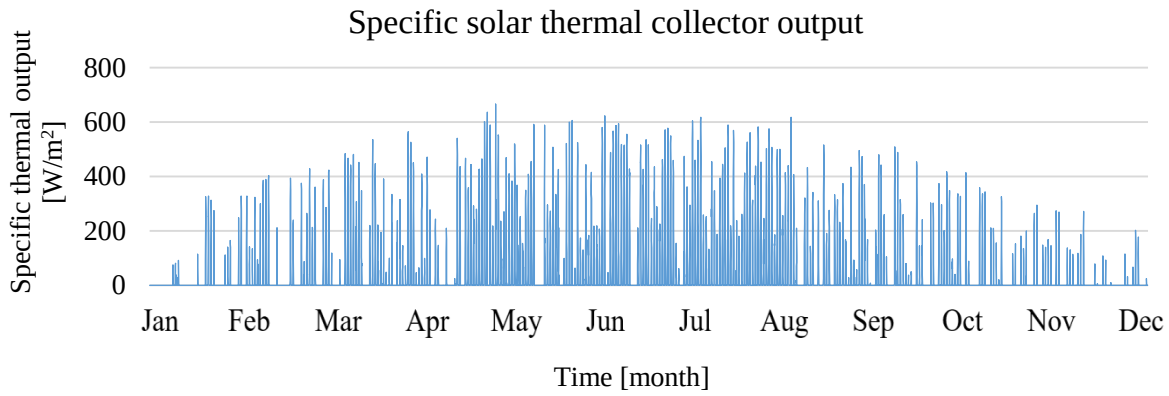

Figure 6 Specific solar thermal collector output

Cogeneration and power-to-heat units are connected to the electricity market. Power-to-heat technologies are buying electricity, while cogeneration units are selling it on the market. In Scenario 1, as explained in Section 3.2, cogeneration units are receiving a sliding feed-in premium, which means that, beside the electricity market price, they are also getting paid the difference between the reference value (RV) and the market price. If the RV is lower than the market price, then the feed-in premium is equal to zero. Since the Croatian legislation hasn't yet adopted a regulation on defining the RV, for the purpose of this research it has been assumed that the RV is equal to 80% of the currently used feed-in tariff for cogeneration plants [54]. Due to this, the proposed reference value is equal to 55 €/MWh. Since Croatia has established a day-ahead electricity market, called CROPEX [55], this data has been used as an input for the optimization model. Figure 7 shows the historical data for year 2017, which are implemented into the model. The average market price is equal to 51,9 €/MWh, which is relatively close to the feed-in premium reference value.

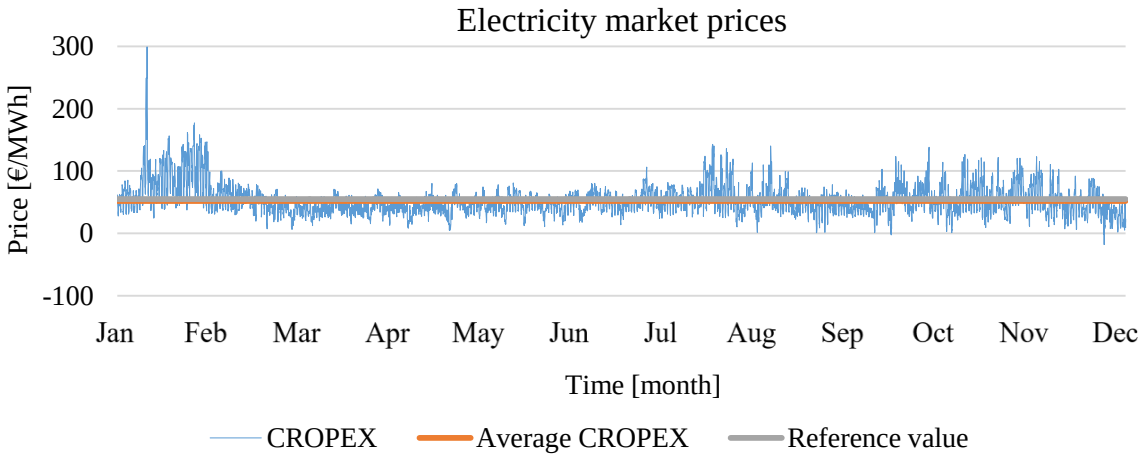

Figure 7 Electricity market prices, CROPEX

Table 1 shows the technology-related data, which consist of the cost (investment, variable and fuel), the emission factor, the efficiency, the ramp-up and ramp-down speed (expressed as share of the total capacity), the technical lifetime and the power-to-heat ratio needed for cogeneration units. All of the data can be found in report [56]. Besides what was previously mentioned, the assumed discount rate is the same for all technologies and is equal to 7%.

As mention in Section 2.3., the exergy factor is needed in order to calculate the exergy input of the fuels, i.e. the exergy destruction of the technology. Two possible fuels are used: natural gas and biomass. The exergy factor of the natural gas is equal to 1,04 while the exergy factor of biomass fuel is equal to 1,2 as shown in papers [35] and [41]. It is important to mention that the exergy factor of biomass depends on the biomass type and water content. The biomass used in this paper is woodchip with water content equal to 25%. Finally, the exergy factor of the electricity is equal to 1.

Table 1 Technology data

Technology	**Investment cost [€/MW] / [€/m²] /[€/MWh]**	**Fuel cost [€/MWh]**	**Variable cost [€/MWh]**	**Emission factor [TCO_2/MWh]**	**Efficiency/ storage loss [-]**	**Ramp-up/down [-]**	**Technical lifetime [years]**	**Power-to-heat ratio [-]**
Natural gas boiler	100.000	20	3	0,22	0,9	0,7	35	-
Biomass boiler	800.000	15	5,4	0,04	0,8	0,3	25	-
Electrical heater	107.500	Electricity market	0,5	0,234	0,98	0,95	20	-
Heat pump	680.000	Electricity market	0,5	0,234	Hourly distribution	0,95	20	-
Cogeneration natural gas	1.700.000	20	3,9	0,22	0,5 (thermal)	0,3	25	0,82
Cogeneration biomass	3.000.000	15	5	0,04	0,6 (thermal)	0,3	20	0,55
Solar thermal	300 €/m²	0	0,5	0	Hourly distribution	-	25	-
Thermal storage, buffer	3.000 €/MWh	0	0	0	1% (loss)	-	25	-
Seasonal thermal storage	500 €/MWh	0	0	0	0,1% (loss)	-	25	-

3.2. Scenario analysis

For the purpose of this research, two scenarios are proposed. In Scenario 1, i.e. the Reference Scenario, the electricity market prices are equal to those shown in Figure 7, while cogeneration units receive a sliding feed-in premium. In Scenario 2, the electricity market prices are lowered by 30%, thus achieving an average market price equal to 36,4 €/MWh. Furthermore, in this scenario cogeneration units do not receive a feed-in premium, thus achieving lower profit.

4. Results and discussion

The proposed model was written in an open-source and free programming language called Julia [57]. Since the problem falls into the domain of linear programming, an LP solver was used, called Clp [58]. It is a free and open-source optimization coin-or branch and cut solver that is part of the JuMP package [59] used for mathematical optimization. The process of obtaining a single Pareto point lasted around 30 minutes. After the first few runs where weighted factors were varied, the Pareto surface was completed by using the epsilon constraint method. The optimizations were run on a laptop with Intel Core i7.

4.1. Scenario 1 – reference electricity market prices

4.1.1. Pareto surface

The final results are shown in Figure 8, where the blue points represent Pareto solutions forming a Pareto front. There are three points, which are the boundaries of the Pareto surface and are shown in Table 2. The point marked with red represents the least-cost solution, the green point is the most environmentally friendly solution, while the purple point represents the Pareto solution with the least

exergy destruction. The lowest possible discounted cost is equal to 646.551 EUR, the lowest possible CO_2 emissions are equal to 1.111 tonnes, while the lowest exergy destruction is 10.909 MWh. Furthermore, these are the coordinates of the perfect, but unreachable, solution called the Utopia point which is marked with orange colour in Figure 8.

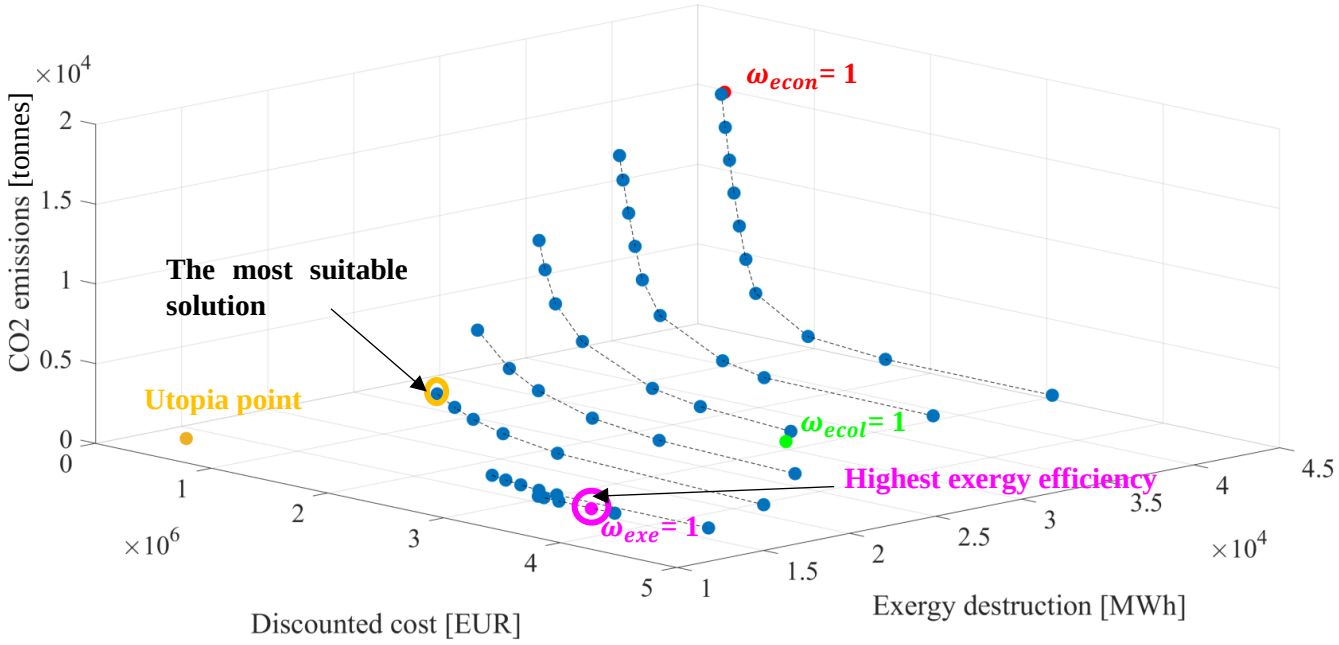

Figure 8 Solution of multi-objective optimization

Table 2 Optimal values of objective functions and calculated exergy efficiency

	$f_{econ_{\omega_{econ}=1}}$	$f_{ecol_{\omega_{ecol}=1}}$	$f_{exe_{\omega_{exe}=1}}$
Total discounted cost [EUR]	646.551	3.197.236	4.130.740
Total exergy destruction [MWh]	42.186	28.521	10.909
Total carbon dioxide emissions [tonnes]	16.108	1.111	2.135
Exergy efficiency [-]	0,45	0,47	0,69

The supply capacities for Pareto solutions shown in Table 2 are presented in Table 3. The least-cost solution utilizes natural gas as fuel in a 7,4 MW heat-only boiler and a 5,7 MW cogeneration unit in combination with 146 MWh of buffer thermal storage. Cogeneration operates through a whole year, since it achieves an additional income, as shown in Equation (1), while a heat-only boiler is used during the colder winter months. The solution with the lowest CO_2 emissions utilizes the maximum available solar thermal collector area, which is set to 50.000 m^2, and a 17,5 MW biomass boiler. It is important to note that a heat-pump isn't part of this solution since it uses electricity as a fuel which also has carbon dioxide emissions due to the fuel mix in the power sector.

This is one of the major drawbacks of this method, since it optimizes the system for a reference year and could potentially cause a lock-in effect in the energy system. Lock-in effect in the energy system implies that decision has to be done without knowing which parameters will change in the future. In this case, various supply capacities have to be installed by taking into account only reference year data. However, these installed supply capacities will have to operate for next 20-30 years, while different parameters which influence their operation could change drastically. We say that the system is then "locked", i.e. it has to operate outside its optimal point. A further decrease in carbon footprint of the power sector is to be expected in the following years, which will make heat pumps more

environmentally friendly. Furthermore, future integration of variable renewable energy sources will also potentially lower electricity market prices thus decreasing operational cost of the heat pumps and making them more economically feasible.

Finally, the technologies utilized in the least-exergy destruction solution is a 18,7 MW heat pump and the maximum solar thermal collector area in combination with seasonal thermal storage with the capacity of 3.878 MWh. This solution also has an extremely high cost, as seen in Figure 8. The reason for this is the necessity for installing capacities with a high investment cost in order to minimize exergy destruction.

Table 3 Supply capacities for solutions where objective functions reach minimum values

Supply capacity / Thermal storage capacity	$f_{econ}{}_{\omega_{econ}=1}$	$f_{ecol}{}_{\omega_{ecol}=1}$	$f_{exe}{}_{\omega_{exe}=1}$
Natural gas heat-only boiler [MW]	7,4	0	0
Biomass heat-only boiler [MW]	0	17,5	0
Electrical heater [MW]	0	0	0
Heat pump [MW]	0	0	18,7
Natural gas CHP [MW]	5,7	0	0
Biomass CHP [MW]	0	0	20
Solar thermal collectors area [m^2]	0	50.000	50.000
Short-term thermal storage [MWh]	146	8,7	14
Seasonal thermal storage [MWh]	0	3.883	3.878

4.1.2. Solution with the highest exergy efficiency

As mentioned in Section 2.3, exergy destruction was chosen as an objective function, while efficiency is only a calculated parameter. The solution with the highest exergy efficiency, as shown in Figure 8 marked with a purple circle, achieves the exergy efficiency equal to 0,69. The reason for such high exergy efficiency is the utilization of the maximum amount of solar thermal collectors in combination with seasonal thermal storage and a large-scale heat pump. It is important to mention that this solution is also the one with the lowest exergy destruction.

4.1.3. The most suited solution – supply capacities

Although all Pareto solutions are treated equally, the end-user should define which one is the most suitable, by using a decision-making method. The most suitable solution, chosen according to the method explained in Section 0, is also shown in Figure 8. It is the Pareto point closest to the Utopia point and is marked with an orange circle. It achieves the total discounted cost equal to 1.755.246 EUR, 4.112 tonnes of CO_2 emissions and an exergy destruction equal to 18.000 MWh. The calculated exergy efficiency is equal to 0,31. The optimized supply capacities are shown in Table 4. It utilizes a 11 MW natural gas boiler, a 5,5 MW heat pump in combination with a 5.521 m^2 solar collectors area.

Table 4 Characteristics of the most suitable solution

The most suitable solution	
Supply capacity / Thermal storage capacity	
Natural gas heat-only boiler [MW]	11,0
Biomass heat-only boiler [MW]	0
Electrical heater [MW]	0
Heat pump [MW]	5,5
Natural gas CHP [MW]	0
Biomass CHP [MW]	0
Solar thermal collectors area [m^2]	5.521
Short-term thermal storage [MWh]	30,6
Solar thermal storage [MWh]	61,6
Objective functions values	
Total discounted cost [EUR]	1.755.246
Total exergy destruction [MWh]	18.000
Total carbon dioxide emissions [tonnes]	4.112
Exergy efficiency [-]	0,31

4.1.4. The most suited solution – hourly operation

Hourly operation of a district heating system for a whole year is shown in Figure 9 and Figure 10. It can be seen that the heat pump operates through the whole winter period, while the natural gas boiler is used as a peak unit. During the summer season, domestic hot water demand is covered with solar thermal collectors and storage. Smaller thermal storage serves as a buffer during the winter season and is kept on a technical minimum during the summer season. The hourly district heating load isn't shown in Figure 9 in order to display the supply technology operation more clearly. Furthermore, a more detailed hourly operation of a district heating system for a single winter week is shown in Figure 11 and Figure 12. Seasonal storage does not operate during the presented winter week and because of that isn't shown in Figure 12. The hourly operation of supply capacities (solar thermal collectors) and seasonal thermal storage during a single summer week is shown in Figure 13 and Figure 14, respectively. The hourly operation of buffer thermal storage isn't shown in Figure 14 since it is kept on a technical minimum.

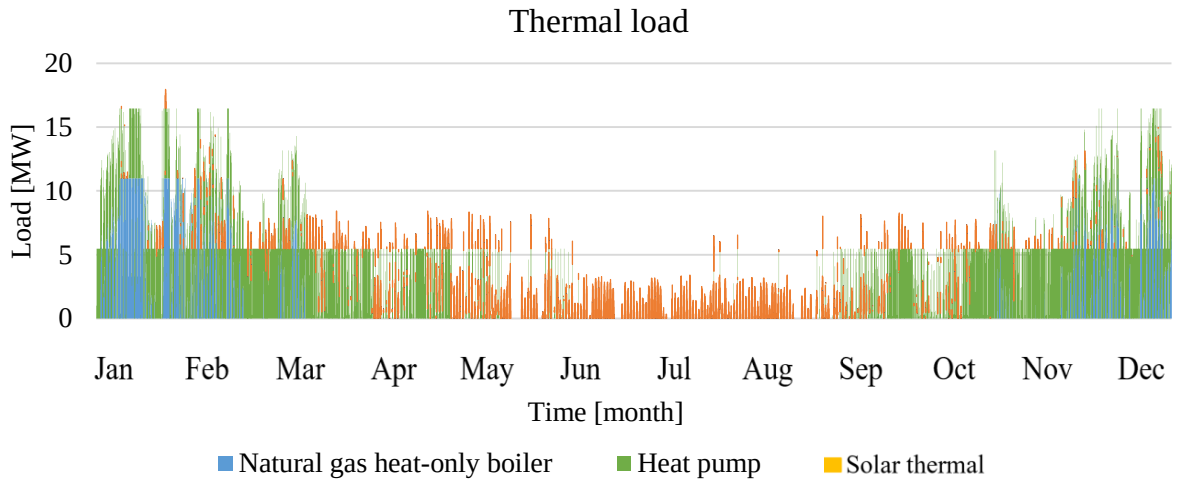

Figure 9 Supply capacities operation of the most suitable solution for a whole year

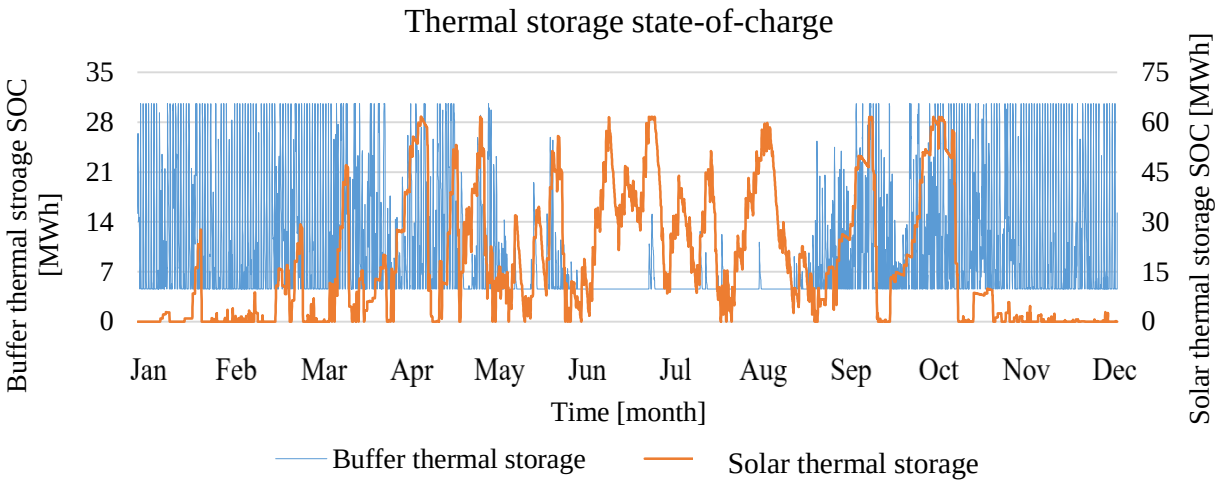

Figure 10 Thermal storage operation of the most suitable solution for a whole year

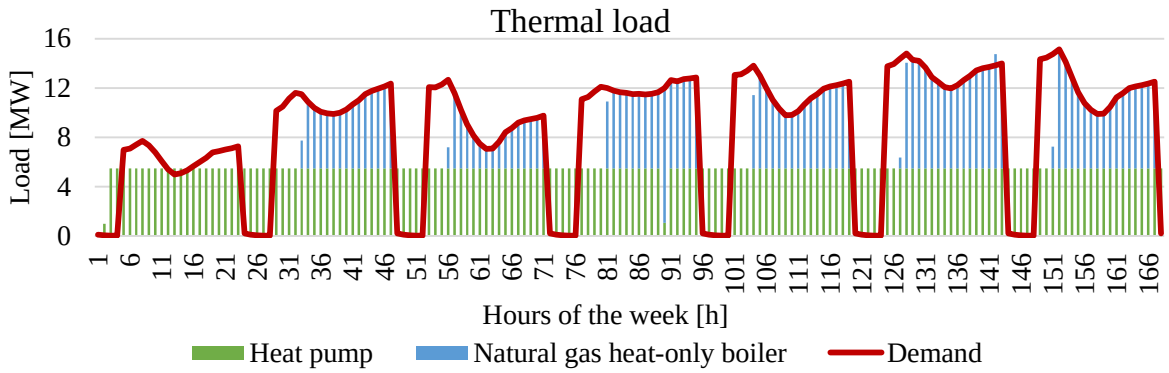

Figure 11 Supply capacities operation of the most suitable solution for a winter week

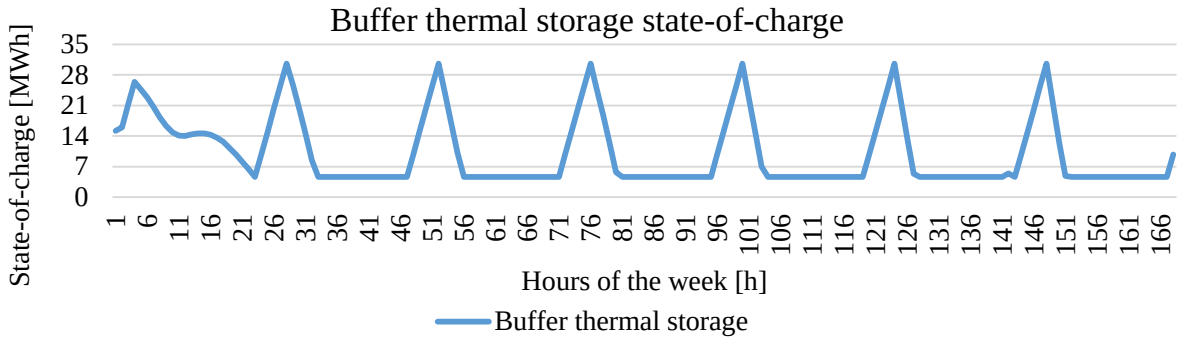

Figure 12 Thermal storage operation of the most suitable solution for a winter week

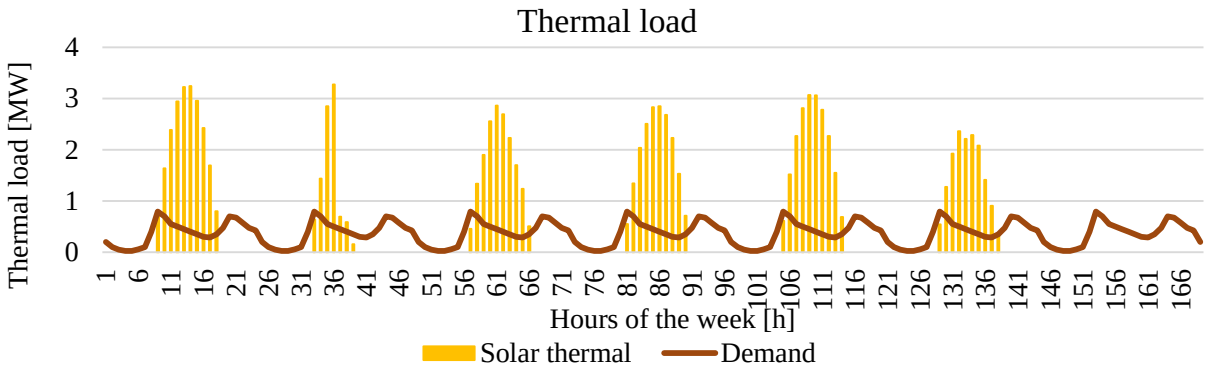

Figure 13 Supply capacities operation of the most suitable solution for a summer week

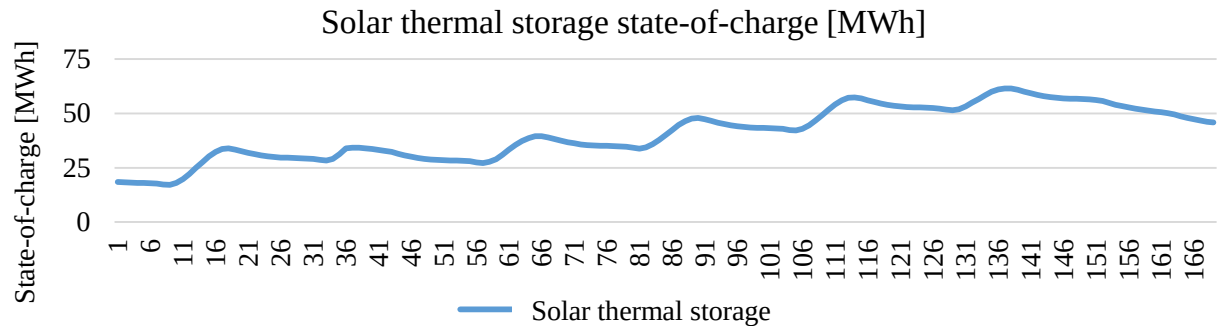

Figure 14 Thermal storage operation of the most suitable solution for a summer week

4.2. Scenario 2 – lower electricity market prices

4.2.1. Pareto frontier comparison

Figure 15a and Figure 15b show Pareto frontiers obtained for Scenario 1 and Scenario 2. Due to the fact that comparison and visualization of two Pareto surface is challenging, 2D diagrams were used in order to compare two scenarios since they are easier to follow and easier to obtain the main conclusion. As explained in the section Case study, Scenario 2 considers reduction of electricity market prices for 30% and an absence of a feed-in premium for cogeneration units. Figure 15a is actually 2D representation of Figure 8. In Figure 8, exergy destruction objective function is shown on additional axis (3D diagram), while in Figure 15a, exergy destruction is a parameter treated as a constant for which Pareto fronts for other two objective functions are plotted in 2D diagram. Pareto fronts in Figure 15a can be understood as slices of the Pareto surface shown in Figure 8. Exergy destruction values shown in Figure 15 are actually epsilon constraints put on exergy destruction objective function. As explained in the section Method, epsilon constraint method has been used in order to obtain equally distanced Pareto points and to visualize the Pareto surface.

First of all, it should be mentioned that the shape of Pareto fronts in a case of objective function minimization is usually similar to that shown in Figure 15, as reported in numerous papers dealing with multi-objective optimization [40], [42], [60], [61]. Therefore, it is to be expected that trends of Pareto fronts obtained in this paper for two different scenarios will have similar shape.

Although Pareto fronts obtained for both scenarios have similar trends, there are crucial differences between two presented scenarios. It can be noticed that Scenario 1 in the region of lower discounted cost achieves higher CO_2 emissions. The main reason for this is utilization of cogeneration units which are preferred due to the higher electricity market prices and existence of a feed-in premium. Although cogeneration units have higher exergy efficiency than heat-only boilers, they emit more CO_2 per MWh

of heat produced. This is also the reason why Scenario 1 obtains lower total discounted cost, in the region where cogeneration units are used. However, in the region where exergetic objective function dominates (exergy destruction lower than 24.000 MWh), values of other two objective functions obtain similar values, both for Scenario 1 and Scenario 2. The main reason for this is utilization of similar technologies and capacities, as shown in Section 4.2.2. This means that electricity market prices have low impact on multi-objective optimization results in the region of low exergy destruction and low environmental impact of the district heating system. However some differences are evident in the region of low exergy destruction. For example, it can be noticed that Pareto fronts for exergy destruction equal to 11.000 MWh obtain different values of total discounted cost in Scenario 1 and Scenario 2. For Scenario 1 it is in range of 3.600.000 EUR up to the 4.300.000 EUR, while in Scenario 2 the range is much smaller, 3.400.000-3.550.500 EUR. As explained in Section 4.2.2., in this region, both scenarios have identical supply capacities, i.e. heat pump is dominant technology. Since Scenario 2 has lower electricity market price, total running cost of the system are also lower. However, in this region carbon dioxide emission are identical and are around 2.160 tonnes of CO_2

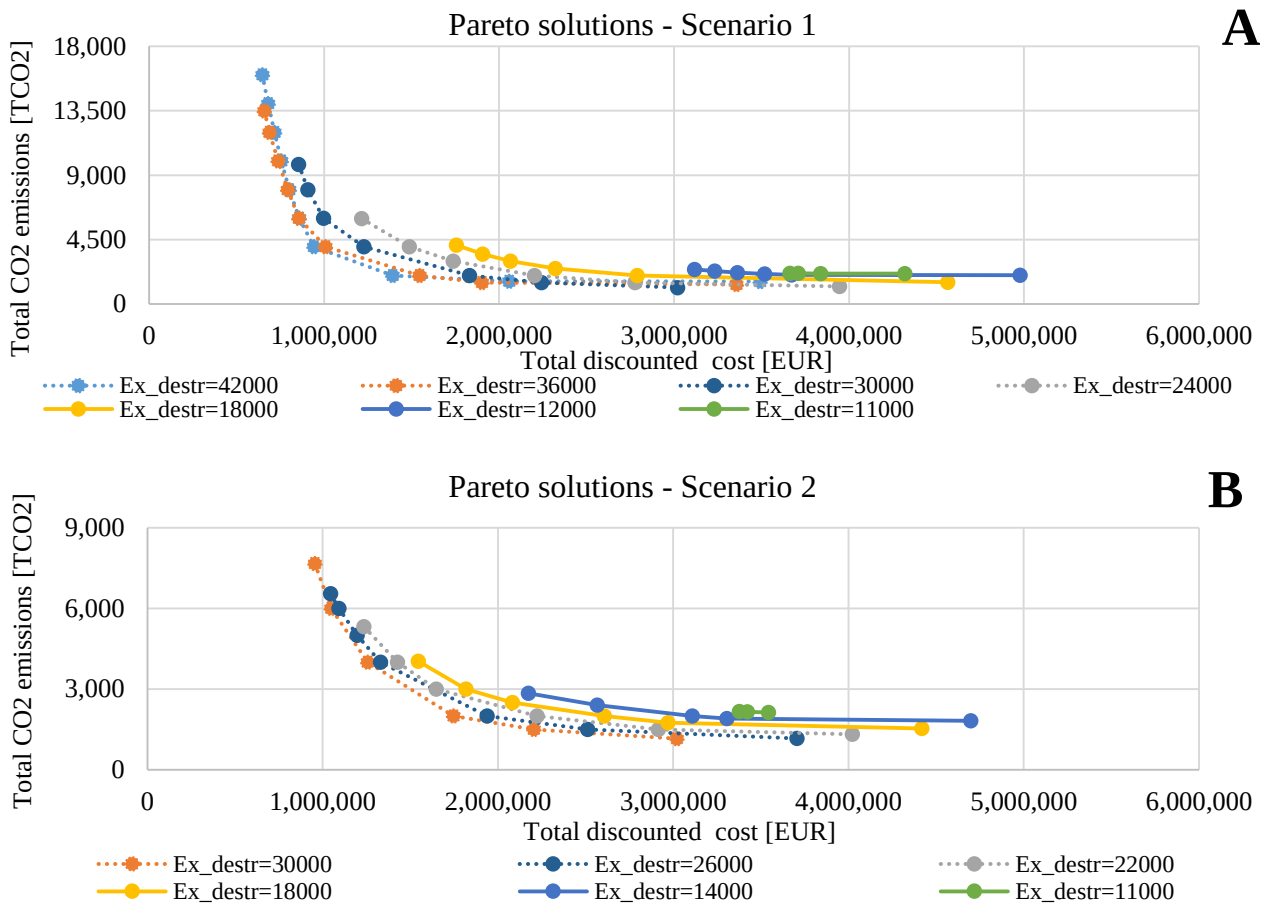

Figure 15 Comparison of Pareto optimal solutions: a) Scenario 1, b) Scenario 2

When comparing Pareto fronts obtained for Scenario 1 and Scenario 2, it can be concluded that there are three noticeable regions. The first one is region of high exergy destruction (around 30.000 MWh) and low discounted cost. In this region, Scenario 1 obtains higher carbon dioxide emissions but achieves lower exergy destruction. The main reason for this is utilization of cogeneration units due to the existence of feed-in premium incentives and higher electricity market prices. The supply capacities trends for this region are shown in Figure 16. The second region is so called “transitional region”, where exergy destruction is around 18.000 MWh. Total cost and carbon dioxide emissions obtain similar values in both scenarios. Furthermore, the trend of supply capacities for this region are shown in Figure

17. It can be noticed that supply capacity trend is similar but not identical. The third region is where both scenarios reach the lowest values of exergy destruction (around 11.000 MWh). In this region, both scenarios have identical supply capacities, which are mostly based on heat pump utilization. Trend of supply capacities for this region is shown in Figure 18.

4.2.2. Supply capacities comparison

Figure 16, Figure 17 and Figure 18 show comparison of supply capacities of Scenario 1 and Scenario 2 for different values of exergy destruction. As explained in Section 4.2.1., there are three regions of interest which will be discussed here in more detail. The first one is region of high exergy destruction (around 30.000 MWh). The second region is so-called transitional region with exergy destruction around 18.000 MWh. The third region is where exergy destruction is almost minimal, i.e. around 11.000 MWh. Each of the mentioned regions is represented in the figures shown below. In order to understand following results, it is important to recall that each Pareto point shown in Figure 15 contains various set of information such as: optimal supply capacities, optimal thermal storage size, optimal hourly operation of the system and calculated exergy efficiency.

In order to describe visualization of the results, supply capacities in Figure 16 are explained in more detail. For both scenarios, three results are shown: optimal supply capacities (top diagrams), calculated exergy efficiency (diagrams in the middle) and optimal thermal storage size (diagrams at the bottom). Left side of diagrams shown in Figure 16, represent solutions where economical objective function is dominant, while right side of the diagrams show solutions where minimization of carbon dioxide emissions is dominant objective function. For example, first supply capacities shown on the left side of the diagram in Figure 16 represent the most left Pareto solution for exergy destruction value equal to 30.000 MWh. The most right capacities shown in Figure 16 represents the most right Pareto solution for exergy destruction value equal to 30.000 MWh. This has also been visualized by connecting mentioned Pareto points with respected information for both scenarios.

As said previously, Figure 16 shows DH system information for exergy destruction equal to 30.000 MWh. Although Scenario 1 and Scenario 2 achieve the same exergy destruction values, Scenario 1, due to higher electricity market values and feed-in premium also utilizes cogeneration units. On the left side of the diagram, where economical objective function is dominant, natural gas is used. It is substituted with biomass cogeneration once approaching the right side of the diagram, where environmental objective function is dominant. In the region where cogeneration is used, Scenario 1 has higher exergy efficiency. When approaching more environmentally friendly solutions, installed capacities, are becoming similar in both scenarios. In this region, both scenarios prefer to use maximum available capacity of solar thermal collectors. Buffer thermal storage is bit higher in Scenario 1 if CHP, which has lower ramp-up and ramp-down rates, is used. Exergy efficiency in Scenario 2 is gradually increasing from 0,18 up to 0,45. It can be noticed that increase of exergy efficiency follows installed solar thermal collector area. Furthermore, seasonal thermal storage size follows the solar thermal collector area.

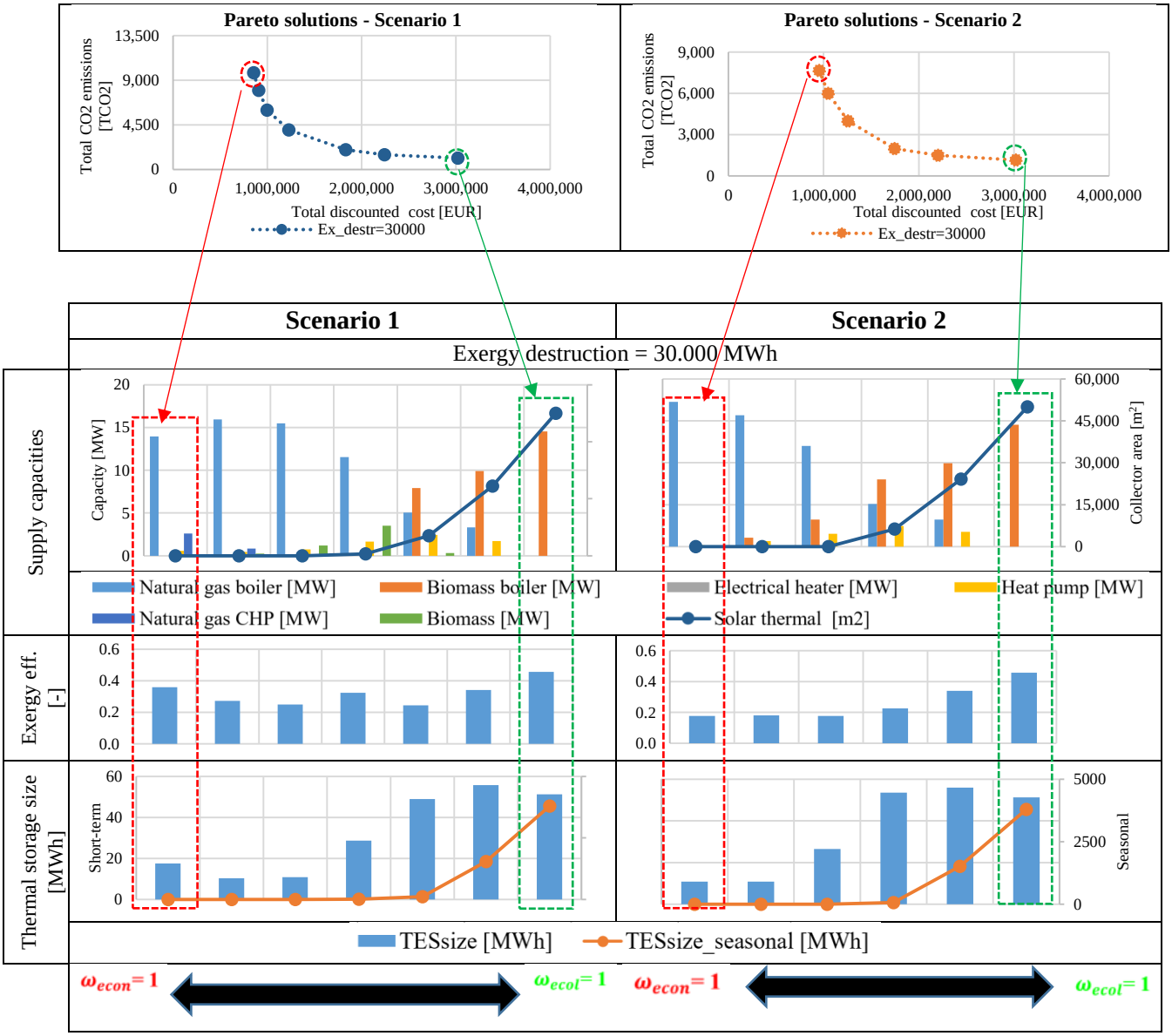

Figure 16 Comparison of supply capacities for exergy destruction equal to 30.000 MWh

Figure 17 show comparison of supply capacities for two scenarios but for exergy destruction value equal to 18.000 MWh. As mentioned in the Section 4.2.1. it can be seen that both scenarios have similar optimal supply capacities. At the left side of the diagram heat pump in combination with natural gas and solar thermal collectors is used. When approaching the left side of the diagram, where environmental objective function is dominant, biomass heat-only boiler has replaced natural gas. Furthermore, solar thermal collector area has reached maximum value. It is important to notice that solar thermal collectors are not utilized only in the most environmentally friendly solution, but are gradually increased together with seasonal thermal storage size. The trend of solar thermal collector area differs between two scenarios. In Scenario 1, it increases almost exponentially, while in Scenario 2 it has saturation effect.

As already mentioned in Section 4.2.1, Pareto solutions in the region of low exergy destruction obtain identical optimal supply capacities in both scenarios. This can also be seen in Figure 18, which shows optimal supply capacities for, relatively low exergy destruction equal to 11.000 MWh. It can be noticed that heat pump is dominant solution, while other technologies have low capacity and operate as the peak technology units. The lowest heat pump capacity is equal to 13 MW, while the highest heat pump

capacity is equal to 16,9 MW. Furthermore, it can be noticed that in this region, solar thermal collectors have maximum installed area, even for the least cost solution. Exergy efficiency in this region is relatively high, around 0,65, due to the high solar thermal production. Finally, it can be noticed that electrical heater has also been included as the optimal solution in this region, operating as the peak unit.

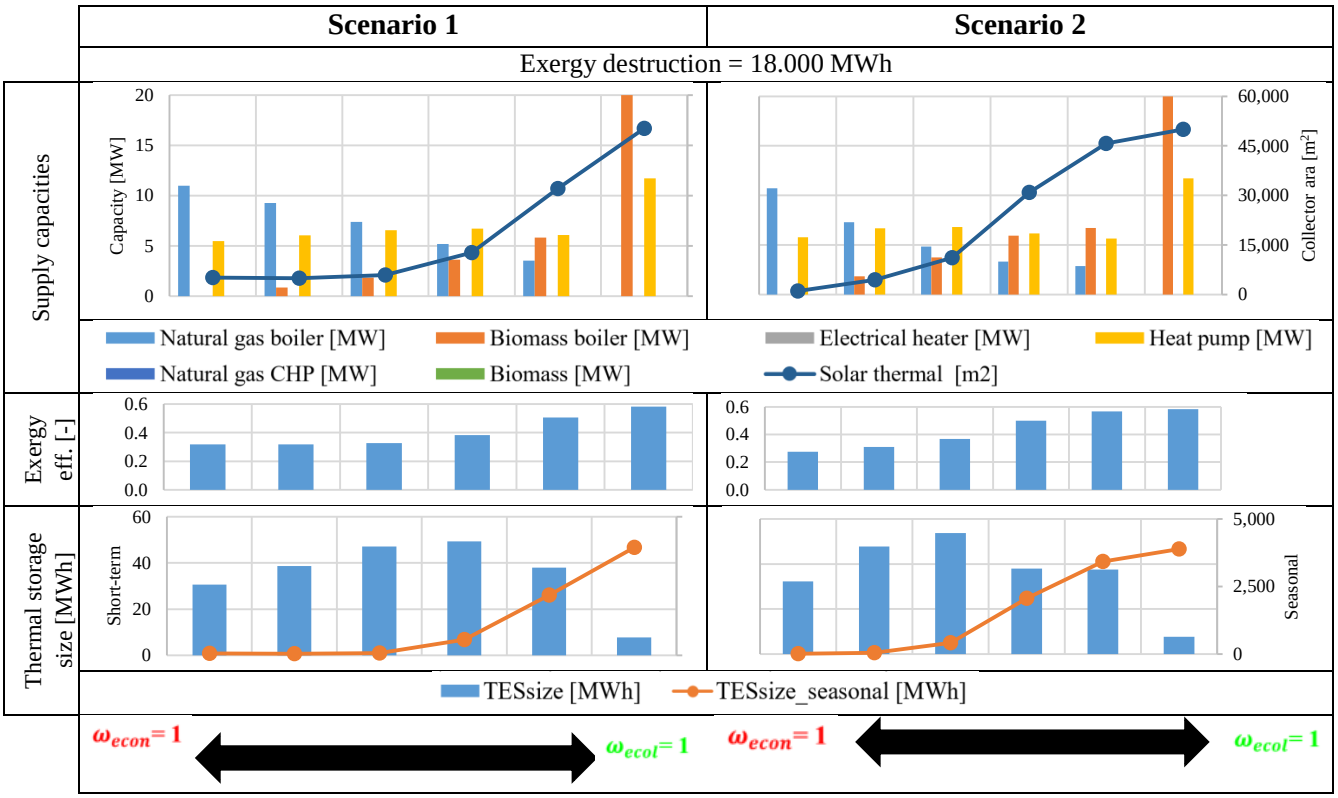

Figure 17 Comparison of supply capacities for exergy destruction equal to 18.000 MWh

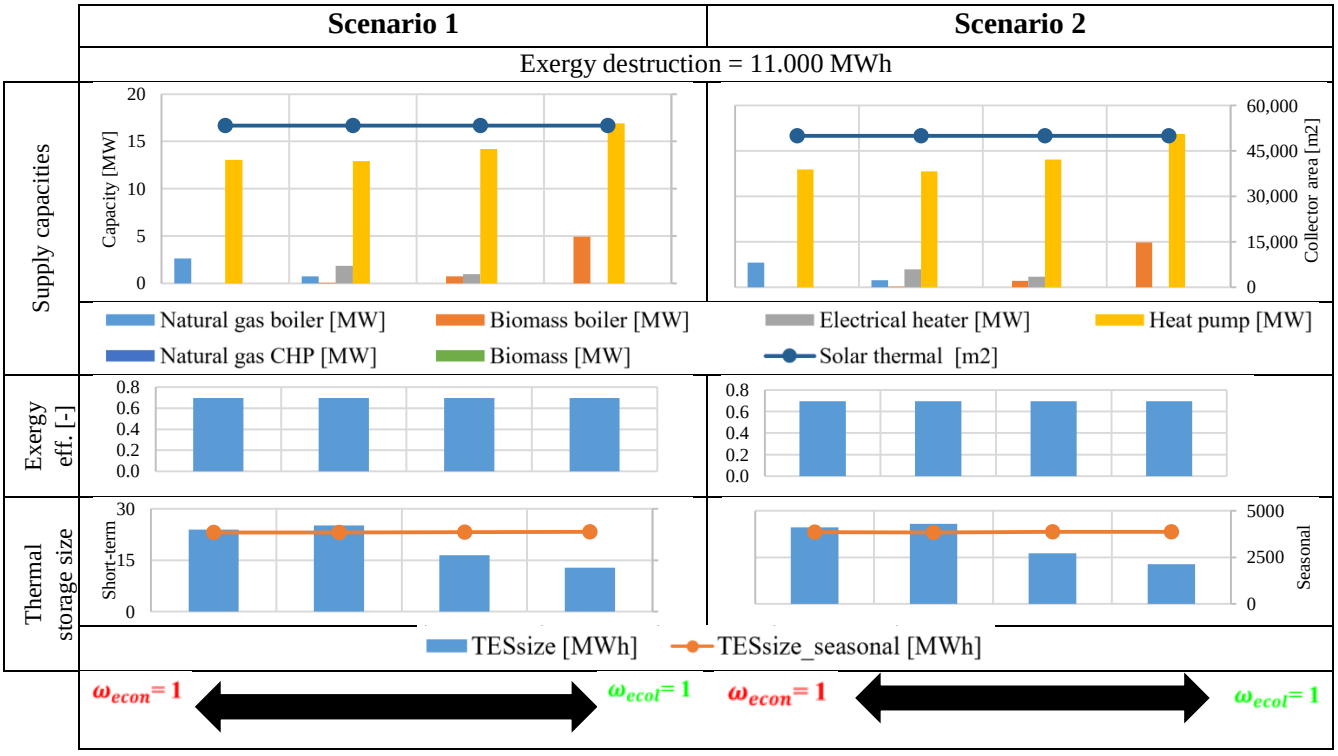

Figure 18 Comparison of supply capacities for exergy destruction equal to 11.000 MWh

4.3.Natural gas technologies phase-out

Natural gas as a fuel, from the exergetic point of view, shouldn't be used for thermal energy production in heat-only boiler units, due to great exergy destruction. The results acquired in this paper also lead to this conclusion. Figure 19 and Figure 20 show optimal natural gas fuelled capacities as a part of the least-cost solution for different exergy destruction values of Scenario 1. These capacities belong to the Pareto points in Figure 8 with the lowest total discounted cost for different exergy destruction values, i.e. these solutions are located at the most-left side of the diagram. It can be seen that the optimal capacity of a natural gas heat-only boiler drops as exergy destruction decreases. This is especially visible in Scenario 2 where, due to the low electricity market prices, a natural gas cogeneration unit hasn't been chosen as a part of any least-cost solutions. The phase-out of the natural gas heat-only boiler in Scenario 1 isn't that obvious, since the maximum optimal capacity isn't reached for the maximum exergy destruction value. The main reason for this is a gradual replacement of natural gas cogeneration. In the systems with low exergy destruction, natural gas operates with a relatively low load factor and acts as a peak boiler solution. For example, for an exergy destruction value equal to 18.000 MWh, the load factor of a natural gas boiler is 10%. For the lowest possible exergy destruction, natural gas isn't used as fuel. As can be seen in Figure 16, Figure 17 and Figure 18, the most-environmentally friendly solutions don't use natural gas a fuel. For these, thermal load is covered by biomass boiler, heat pumps and solar thermal collectors.

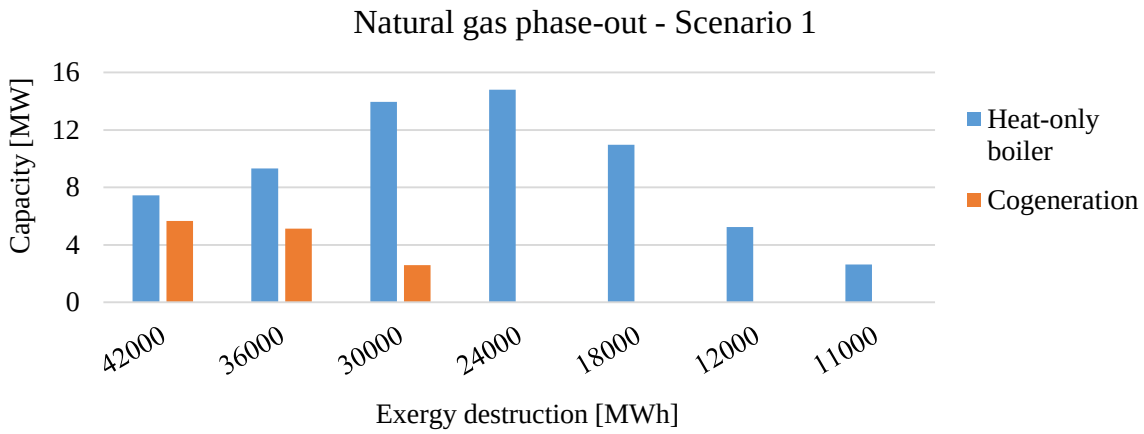

Figure 19 Natural gas fuelled capacities as a part of the least-cost solution for different exergy destruction values, Scenario 1

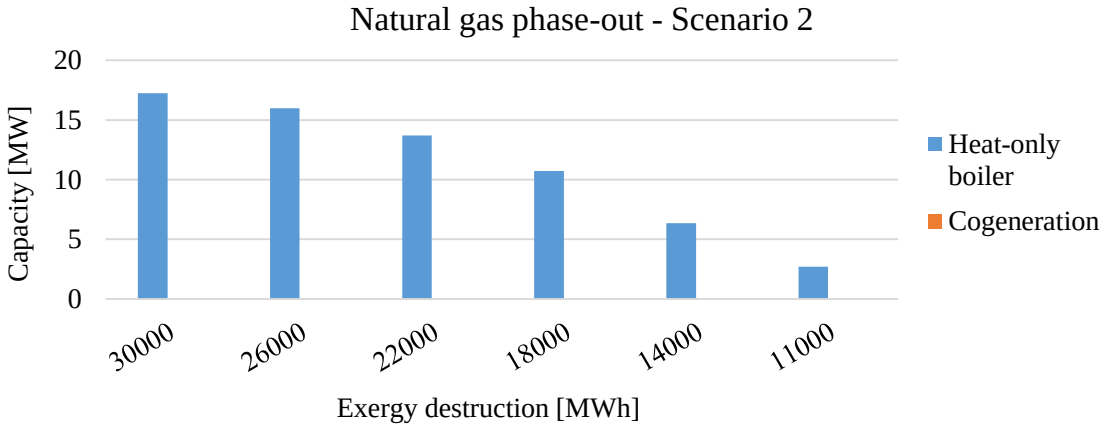

Figure 20 Natural gas fuelled capacities as a part of the least-cost solution for different exergy destruction values, Scenario 2

5. Conclusion

In this paper, a novel method for district heating multi-objective optimization has been proposed. The objective functions are defined as the minimization of total cost, the minimization of the system's carbon dioxide emissions and the minimization of exergy destruction. Two scenarios have been proposed: the first one with reference electricity market prices that also includes the feed-in premium for cogeneration units and the second one, with lower electricity market prices and without a feed-in premium. The obtained results shape the Pareto surface, which displays a compromise between the three objective functions. The most suitable solution for Scenario 1 was defined as the one closest to the Utopia point. It consist of 11 MW natural gas heat only boiler, 5,5 MW heat pump and a 5.521 m^2 of solar thermal collectors area in combination with thermal storage. The reduction of electricity market prices influences the Pareto optimal solutions, especially in the region of a low discounted cost: in Scenario 1 cogeneration units are used, while in Scenario 2 they aren't profitable due to the low electricity market prices. However, in the region where an exergetic objective function is dominant, the optimal supply capacities look identical. This research also shows the phase-out of natural gas based technologies, when approaching the solution with the lowest exergy destruction. The multi-objective optimization of district heating system developed in this paper could be used in future research in order to analyse and define an exergy tax model that could additionally penalize thermal energy production from high temperature sources.

Acknowledgement

Financial support from the RESFLEX project funded by the Programme of the Government of Republic of Croatia, Croatian Environmental Protection and Energy Efficiency Fund with the support of the Croatian Science Foundation for encouraging research and development activities in the area of Climate Change for the period from 2015 to 2016 in the amount of 1.344.100 HRK is gratefully acknowledged.

References

[1] H. Lund *et al.*, "4th Generation District Heating (4GDH). Integrating smart thermal grids into future sustainable energy systems.," *Energy*, vol. 68, pp. 1–11, 2014.

[2] H. Lund, N. Duic, P. A. Ostergaard, and B. V. Mathiesen, "Future District Heating Systems and Technologies : On the role of Smart Energy Systems and 4 th Generation District," *Energy*, 2018.

[3] L. Brange, J. Englund, and P. Lauenburg, "Prosumers in district heating networks - A Swedish case study," *Appl. Energy*, vol. 164, pp. 492–500, 2016.

[4] H. Ahvenniemi and K. Klobut, "Future Services for District Heating Solutions in Residential Districts," *J. Sustain. Dev. Energy, Water Environ. Syst.*, vol. 2, no. 2, pp. 127–138, 2014.

[5] M. A. Sayegh *et al.*, "Trends of European research and development in district heating technologies," *Renew. Sustain. Energy Rev.*, pp. 1–10, 2016.

[6] A. Lake, B. Rezaie, and S. Beyerlein, "Review of district heating and cooling systems for a sustainable future," *Renew. Sustain. Energy Rev.*, vol. 67, pp. 417–425, 2017.

[7] S. Frederiksen and S. Werner, *District Heating and Cooling*. 2013.

[8] M. Gong and S. Werner, "Exergy analysis of network temperature levels in Swedish and Danish district heating systems," *Renew. Energy*, vol. 84, pp. 106–113, 2015.

[9] H. Li and S. Svendsen, "Energy and exergy analysis of low temperature district heating

network," *Energy*, vol. 45, no. 1, pp. 237–246, 2012.

[10] H. Gadd and S. Werner, "Achieving low return temperatures from district heating substations," *Appl. Energy*, vol. 136, pp. 59–67, 2014.

[11] Ş. Kilkiş, "A Rational Exergy Management Model to Curb CO 2 Emissions in the Exergy-Aware Built Environments of the Future," KTH Royal Institute of Technology, Stockholm, Sweden, 2011.

[12] Ş. Kilkiş, "Exergy transition planning for net-zero districts," *Energy*, vol. 92, no. Part 3, pp. 515–531, 2015.

[13] X. Yang, H. Li, and S. Svendsen, "Energy, economy and exergy evaluations of the solutions for supplying domestic hot water from low-temperature district heating in Denmark," *Energy Convers. Manag.*, vol. 122, pp. 142–152, 2016.

[14] I. Baldvinsson and T. Nakata, "A feasibility and performance assessment of a low temperature district heating system e A North Japanese case study," *Energy*, vol. 95, pp. 155–174, 2016.

[15] I. Baldvinsson and T. Nakata, "A comparative exergy and exergoeconomic analysis of a residential heat supply system paradigm of Japan and local source based district heating system using SPECO (specific exergy cost) method," *Energy*, vol. 74, no. C, pp. 537–554, 2014.

[16] N. Yamankaradeniz, "Thermodynamic performance assessments of a district heating system with geothermal by using advanced exergy analysis," *Renew. Energy*, vol. 85, pp. 965–972, 2016.

[17] A. Keçebaş, I. Yabanova, and M. Yumurtaci, "Artificial neural network modeling of geothermal district heating system thought exergy analysis," *Energy Convers. Manag.*, vol. 64, pp. 206–212, 2012.

[18] N. Kabalina, M. Costa, W. Yang, A. Martin, and M. Santarelli, "Exergy analysis of a polygeneration-enabled district heating and cooling system based on gasification of refuse derived fuel," *J. Clean. Prod.*, vol. 141, pp. 760–773, 2017.

[19] Jiangjiang Wang Ying Yang, "Energy, exergy and environmental analysis of a hybrid combined cooling heating and power system utilizing biomass and solar energy," *Energy Convers. Manag.*, vol. 124, pp. 566–577, 2016.

[20] S. a. Kalogirou, S. Karellas, V. Badescu, and K. Braimakis, "Exergy analysis on solar thermal systems: A better understanding of their sustainability," *Renew. Energy*, pp. 1–6, 2015.

[21] A. Lake and B. Rezaie, "Energy and exergy e ffi ciencies assessment for a strati fi ed cold thermal energy storage," vol. 220, no. April 2017, pp. 605–615, 2018.

[22] A. Rijs and T. Mróz, "Exergy Evaluation of a Heat Supply System with Vapor Compression Heat Pumps," *Energies*, 2019.

[23] T. Tereshchenko and N. Nord, "Energy planning of district heating for future building stock based on renewable energies and increasing supply flexibility," *Energy*, vol. 112, pp. 1227–1244, 2016.

[24] R. Mikulandrić *et al.*, "Performance Analysis of a Hybrid District Heating System : A Case Study of a Small Town in Croatia," *J. Sustain. Dev. Energy, Water Environ. Syst.*, vol. 3, no. 3, pp. 282–302, 2015.

[25] J. Skorek, P. Bargiel, and M. Tan, "Energy and economic optimization of the repowering of coal-fired municipal district heating source by a gas turbine," *Energy Convers. Manag.*, 2017.

[26] M. Anatone and V. Panone, "A model for the optimal management of a CCHP plant," *Energy Procedia*, vol. 81, pp. 399–411, 2015.

[27] M. Hu and H. Cho, “A probability constrained multi-objective optimization model for CCHP system operation decision support,” *Appl. Energy*, vol. 116, pp. 230–242, 2014.

[28] T. Falke, S. Krengel, A.-K. Meinerzhagen, and A. Schnettler, “Multi-objective optimization and simulation model for the design of distributed energy systems,” *Appl. Energy*, 2016.

[29] S. Bracco, G. Dentici, and S. Siri, “Economic and environmental optimization model for the design andthe operation of a combined heat and power distributed generation system in an urban area,” *Energy*, vol. 55, pp. 1014–1024, 2013.

[30] X. Zheng *et al.*, “A MINLP multi-objective optimization model for operational planning of a case study CCHP system in urban China,” *Appl. Energy*, 2017.

[31] P. A. Østergaard and A. N. Andersen, “Booster heat pumps and central heat pumps in district heating,” *Appl. Energy*, 2016.

[32] T. Tezer, R. Yaman, and G. Yaman, “Evaluation of approaches used for optimization of stand-alone hybrid renewable energy systems,” *Renew. Sustain. Energy Rev.*, vol. 73, no. June 2016, pp. 840–853, 2017.

[33] W. Jakob and C. Blume, “Pareto Optimization or Cascaded Weighted Sum: A Comparison of Concepts,” *Algorithms*, vol. 7, pp. 166–185, 2014.

[34] A. Franco and F. Bellina, “Methods for optimized design and management of CHP systems for district heating networks (DHN),” *Energy Convers. Manag.*, vol. 172, no. January, pp. 21–31, 2018.

[35] A. Franco and M. Versace, “Optimum sizing and operational strategy of CHP plant for district heating based on the use of composite indicators,” *Energy*, vol. 124, pp. 258–271, 2017.

[36] A. Franco and M. Versace, “Multi-objective optimization for the maximization of the operating share of cogeneration system in District Heating Network,” *Energy Convers. Manag.*, vol. 139, pp. 33–44, 2017.

[37] Y. Z. Wang *et al.*, “Multi-objective optimization and grey relational analysis on configurations of organic Rankine cycle,” *Appl. Therm. Eng.*, 2016.

[38] F. A. Boyaghchi and M. Chavoshi, “Multi-criteria optimization of a micro solar-geothermal CCHP system applying water/CuO nanofluid based on exergy, exergoeconomic and exergoenvironmental concepts,” *Appl. Therm. Eng.*, vol. 112, pp. 660–675, 2017.

[39] H. Lu *et al.*, “Transition path towards hybrid systems in China: Obtaining net-zero exergy district using a multi-objective optimization method,” *Energy Build.*, vol. 85, pp. 524–535, 2014.

[40] M. Di Somma *et al.*, “Operation optimization of a distributed energy system considering energy costs and exergy efficiency,” *Energy Convers. Manag.*, vol. 103, pp. 739–751, 2015.

[41] M. Di Somma *et al.*, “Multi-objective design optimization of distributed energy systems through cost and exergy assessments,” *Appl. Energy*, vol. 204, pp. 1299–1316, 2017.

[42] H. Dorotić, T. Pukšec, and N. Duić, “Multi-objective optimization of district heating and cooling systems for a one-year time horizon,” *Energy*, vol. 169, pp. 319–328, 2019.

[43] T. Tereshchenko and N. Nord, “Implementation of CCPP for energy supply of future building stock,” *Appl. Energy*, vol. 155, pp. 753–765, 2015.

[44] “Programme of Exploiting Heating and Cooling Efficiency Potential for 2016-2030.” .

[45] M. Pavičević, T. Novosel, T. Pukšec, and N. Duić, “Hourly optimization and sizing of district heating systems considering building refurbishment - Case study for the city of Zagreb,” *Energy*, 2016.

[46] N. Nakicenovic, P. V. Gilli, and R. Kurz, “Regional and Global Exergy and energy efficiencies,” *Energy*, vol. 21, no. 3, pp. 223–237, 1996.

[47] A. Ziebik and P. Gładysz, “Optimal coefficient of the share of cogeneration in district heating systems,” *Energy*, vol. 45, no. 1, pp. 220–227, 2012.

[48] JRC, “PVGIS.” [Online]. Available: http://re.jrc.ec.europa.eu/pvgis.html.

[49] “Renewable ninja.” [Online]. Available: https://www.renewables.ninja/.

[50] “SPF Institut für Solartechnik.” [Online]. Available: http://www.spf.ch/index.php?id=111&L=6.

[51] “Odyssee-MURE.” [Online]. Available: http://www.indicators.odyssee-mure.eu/energy-efficiency-database.html.

[52] “Meteonorm.” [Online]. Available: http://www.meteonorm.com/.

[53] P. A. Sørensen, J. E. Nielsen, R. Battisti, T. Schmidt, and D. Trier, “Solar district heating guidelines: Collection of fact sheets,” no. August, p. 152, 2012.

[54] “Croatian Energy Market Operator (HROTE).”

[55] “CROPEX.” [Online]. Available: https://www.cropex.hr/hr/.

[56] D. Heating and E. C. Generation, *Technology data for energy plants*. 2012.

[57] “Julia programming language.” [Online]. Available: https://julialang.org.

[58] “Clp optimization solver.” [Online]. Available: https://projects.coin-or.org/Cbc.

[59] “JuMP.” [Online]. Available: http://www.juliaopt.org/JuMP.jl/0.18/.

[60] T. Falke, S. Krengel, A.-K. Meinerzhagen, and A. Schnettler, “Multi-objective optimization and simulation model for the design of distributed energy systems,” *Applied Energy*. 2016.

[61] D. Xu, M. Qu, Y. Hang, and F. Zhao, “Multi-objective optimal design of a solar absorption cooling and heating system under life-cycle uncertainties,” *Sustain. Energy Technol. Assessments*, vol. 11, pp. 92–105, 2015.